PRODUCTION OF DIRECT PHOTONS AND LEPTONS IN HADRONIC COLLISIONS

I. Mannelli

CERN

Geneva, Switzerland

INTRODUCTION

The field of direct leptons and photon production in hadronic interactior has been studied extensively from several points of view. The production of resonances and the study of their properties, as deduced from decays into lepton pairs or photons, has provided us with a remarkable insight into the fundamental constitu ents of matter. The subject achieved its full splendor during the period 1974-77 with the discoveries of the J/ψ, the T and the associated families of new particles We all expect a full renaissance at the energies of new colliders. Direct production of large mass continuum dilepton has been successfully interpreted in terms of the Drell-Yan[1] model and QCD. The experimental knowledge and the theoretical understanding has reached quite a good level.

Due to the intrinsic difficulty of detecting direct photons against the large background from resonance decay, this important process has been firmly established experimentally only at the time of the 1979 International Symposium on Lepton and Photon Interactions at High Energies. This review is intended to summar ize the new developments on continuum dilepton and photon direct production. Promp single lepton and dilepton resonance production is not covered.

DIRECT PRODUCTION OF CONTINUUM DILEPTON

The basic description of dilepton production in hadronic interactions within the framework of quark-proton models was given by Drell and Yan[1] in terms of electromagnetic annihilation of a quark and an antiquark of the same flavour and colour into a virtual photon, which then decays producing a lepton pair.

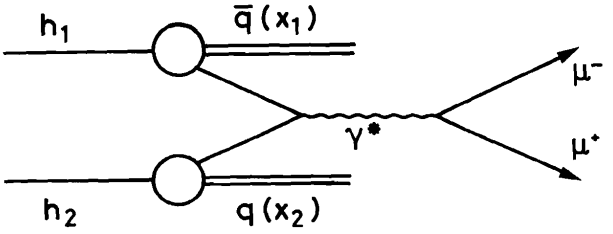

Fig. 1
The basic Drell-Yan diagram

Experiments measure the momenta of the two leptons. Neglecting masses and transverse momenta $M^2_{\mu\mu} = x_1 \cdot x_2 \cdot s$, $x_{\mu\mu} = x_1 - x_2$

$$x_1 = \tfrac{1}{2}(x_{\mu\mu} + \sqrt{x^2_{\mu\mu} + 4M^2_{\mu\mu}/s}) \qquad x_2 = -\tfrac{1}{2}(x_{\mu\mu} - \sqrt{x^2_{\mu\mu} + 4M^2_{\mu\mu}/s})$$

$$\frac{d^2\sigma}{dx_1\,dx_2} = \frac{4\pi\alpha^2}{3sx_1^2x_2^2} \times \frac{1}{3} \times \sum_i Q_i^2 \left\{ f_{q_i}^{h_1}(x_1) \cdot f_{\bar{q}_i}^{h_2}(x_2) + f_{\bar{q}_i}^{h_1}(x_1) \cdot f_{q_i}^{h_2}(x_2) \right\}$$

where $f_q^{h_1}(x_1)$; $f_{\bar{q}}^{h_2}(x_2)$ are the effective quark and antiquark structure functions of projectile and target hadron. Changing variables to M^2 and $x_{\mu\mu}$, since $dM^2_{\mu\mu}\,dx_{\mu\mu} = (x_1 + x_2)s\,dx_1\,dx_2$:

$$\frac{d^2\sigma}{dM_{\mu\mu}^2\, dx_{\mu\mu}} = \frac{4\pi\alpha^2}{3M^4} \times \frac{1}{3} \sum_i \frac{x_1 x_2}{x_1 + x_2} Q_i \left\{ f_{q_i}^{h_1}(x_1)\ f_{\bar{q}_i}^{h_2}(x_2) + f_{\bar{q}_i}^{h_1}(x_1)\ f_{q_i}^{h_2}(x_2) \right\}$$

and since x_1, x_2 depend only on $x_{\mu\mu}$ and on the ratio $\tau = M_{\mu\mu}^2/s$

$$M_{\mu\mu}^3 \frac{d^2\sigma}{dM_{\mu\mu}\, dx_{\mu\mu}} = F_{h_1 h_2}(x_{\mu\mu}, \tau)$$

i.e. the Drell-Yan cross section scales in terms of $x_{\mu\mu}$ and $M_{\mu\mu}/s$. Also, the angular distribution in the dilepton rest mass with respect to the virtual photon direction is supposed to be $\sim 1 + \cos^2\theta$.

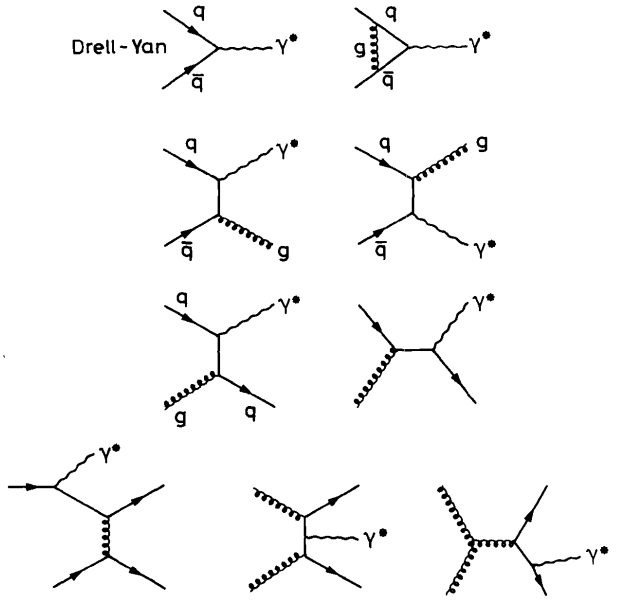

Fig. 2 The basic Drell-Yan diagram and higher order diagrams with gluon exchange or emission.

More elaborate quark-parton models[2] which introduce a non-zero transverse momentum k_T for the quarks and antiquarks in the hadrons and QCD calculations[3] which take into account the emission of virtual and real gluons, Fig. 2, lead to significant changes compared with the Drell-Yan prediction. It is remarkable that the changes with respect to the parton model are in general almost independent of the kinematics and amount to increasing roughly the predictions by a factor $K \simeq 2$. A recent experimental test of the updated Drell-Yan model has been carried out at FNAL by a Michigan-Northwestern-Tufts-Washington University collaboration[4] by comparing cross-sections, calculated using deep inelastic lepton scattering for valence quark distributions as a function of x and q^2 ($= M_{\mu\mu}^2$), with their measurements, shown in Fig. 3, which extend over a large range of $x'_{\mu\mu}$ and $M_{\mu\mu}$.

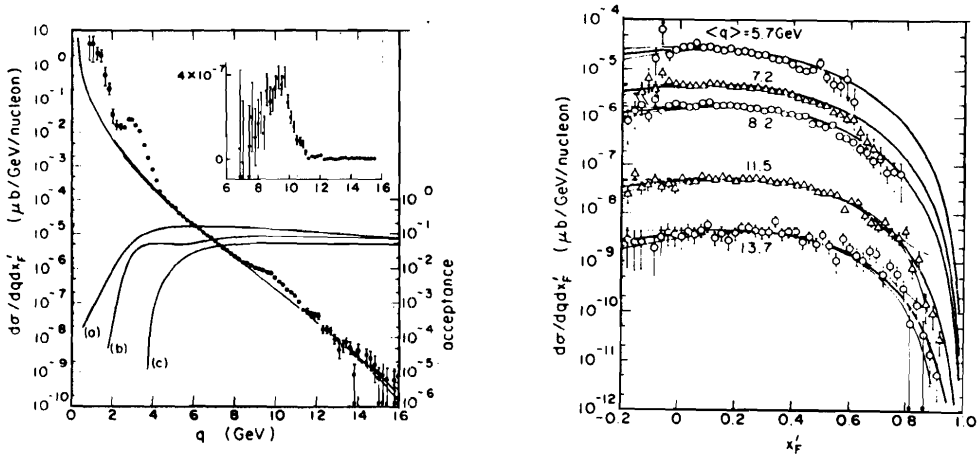

Fig. 3

When the incoming particle contains valence antiquarks, their contribution is generally dominant in collisions against nucleons as can be seen in Fig. 4[5] showing the ratio of dimuon yields for production by π^- and protons and by antiprotons and protons. Figure 5 illustrates the relevance of the charge of the valence antiquark, the π^+/π^- data approaching as expected the value $(1/3\ /\ 2/3)^2 = 0.25$ of the d to $\bar{u}$ charge ratio squared, in the mass region away from resonance contribution.

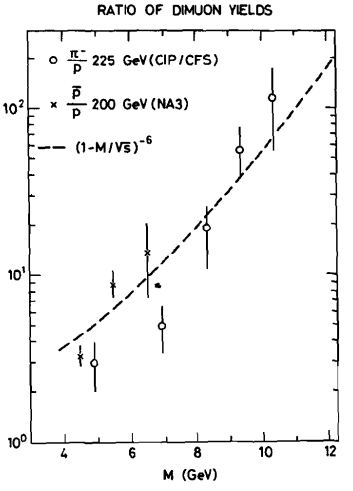

Fig. 4

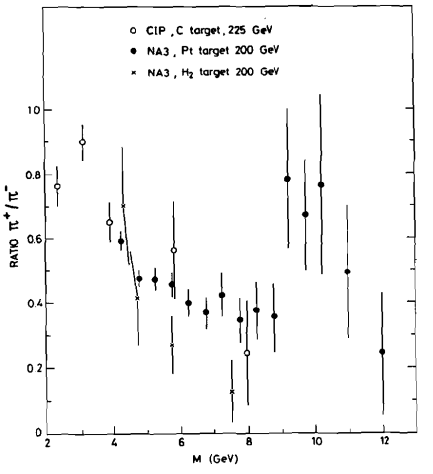

Fig. 5

A large amount of new data has recently become available on the A dependence of dimuon continuum for pion nucleus collisions. Once effects due to Fermi motion, rescattering and difference in structure function between proton and neutrons (important mostly only when comparing hydrogen with other nuclei) are taken into account, the Drell-Yan model simple additivity rule can be tested in a stringent way. Figures 6 and 7 refer to data by the NA3 collaboration, which has the most extensive set of results, and Figs. 8, 9 and 10 and Figs. 11, 12, 13 and 14 to the new detector and first results of the NA10 experiment at CERN and of the CP experiment at FNAL.

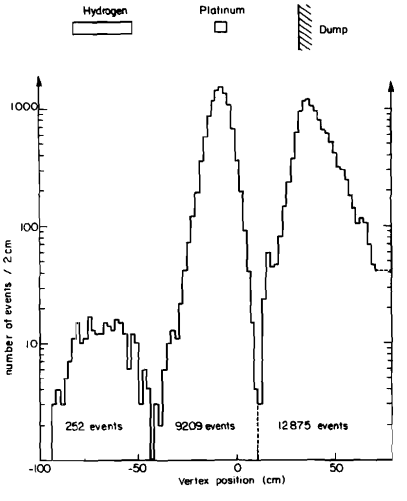

Fig. 6 NA3 collaboration reconstructed vertex position.

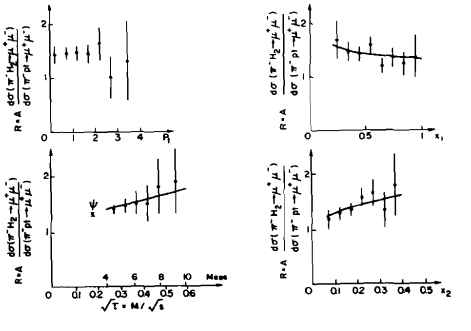

Fig. 7 The full line represents the Drell-Yan prediction after taking into account the appropriate structure functions for protons and neutrons, Fermi motion and re-scattering.

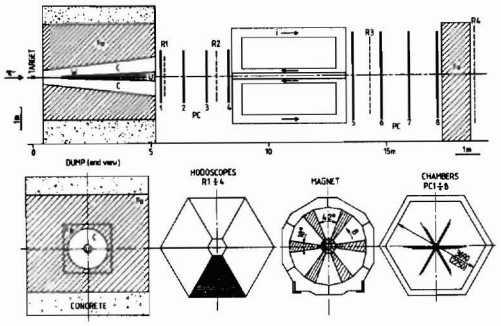

Fig. 8 NA10, schematic of the experimental set-up.

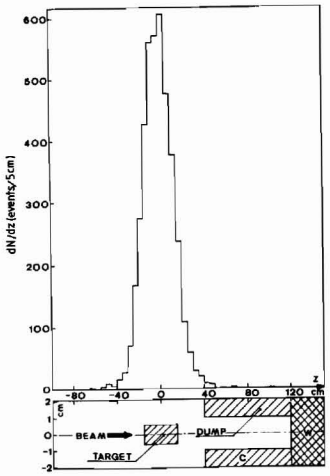

Fig. 9 NA10, reconstructed vertex position.

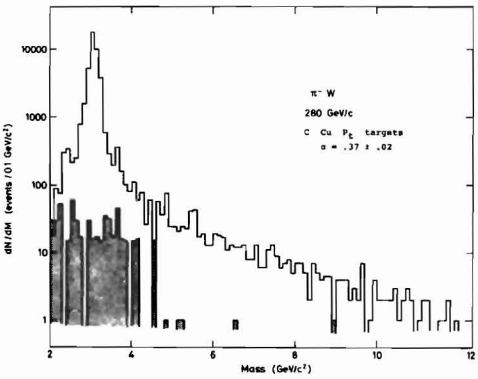

Fig. 10 NA10, μ-pairs mass spectrum. The shaded area refers to like-sign μ-pairs.

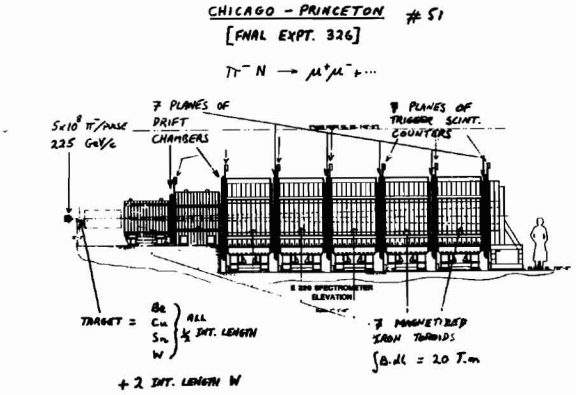

Fig. 11

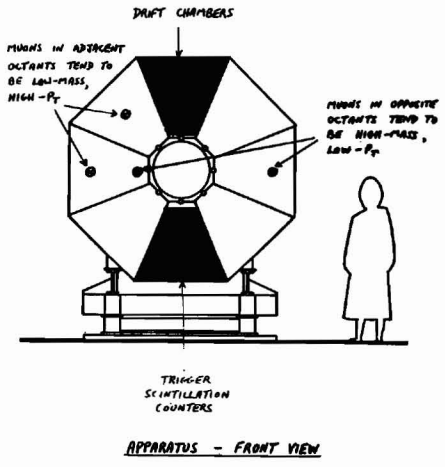

Fig. 12

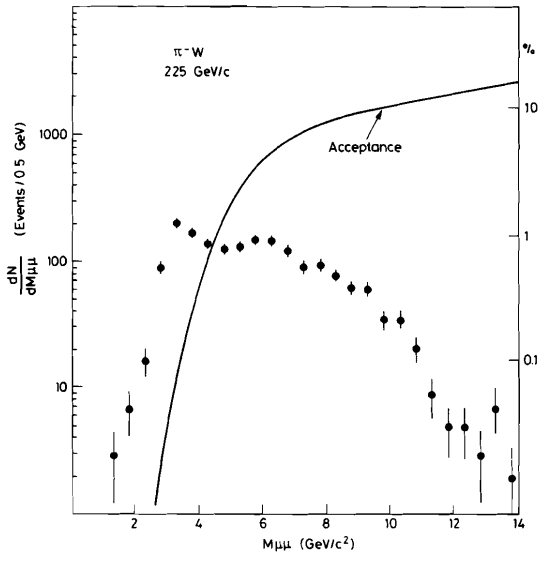

Fig. 13 CP experiment - measured mass spectrum.

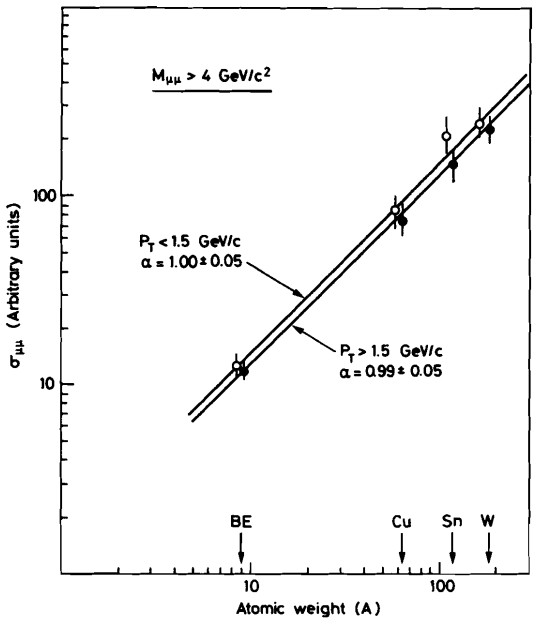

Fig. 14 CP experiment - A dependence.

Table 1 gives an overall summary of the data which are in very good agreement with the Drell-Yan expectation.

Table 1 - Summary π N data

$$\sigma_A = \sigma_0 (Z/A) \cdot A^{\alpha}$$

NA3

	P_{inc}	α	
π^-	200 GeV/c	1.02 ± .03	targets $H_2 \div P_t$
π^-	200 "	.95 ± .04	
$\pi^- - \pi^+$	200 "	1.03 ± .05	
π^-	150 "	1.00 ± .02	
π^-	280 "	1.00 ± .02	
π^-	280 "	.97 ± .05	$C \div P_t$

Drell-Yan
π structure function NA3
N structure function CDHS

NA10 $C \div Cu \div P_t$ targets

	P_{inc}	α	
π^-	280 GeV/c	.97 ± .02	All P_T
α vs P_T		.95 ± .04	$0 \leq P_T \leq 1$ GeV/c
		.99 ± .04	$1 \leq P_T \leq 2$ "
		.97 ± .08	$P_T > 2$ "

CP Be ÷ Cu ÷ Sn ÷ W targets

π^-	225 GeV/c	1.00 ± .05	$0 \leq P_T \leq 1.5$ GeV/c
		.99 ± .05	$P_T \geq 1.5$ "

As far as the A dependence as a function of P_T is concerned, a more elaborate QCD estimate has been derived by C. Michael[6], which, however, remains quite close to the naive $\alpha = 1$ value. It is presented in Fig. 15 together with results of a recent reanalysis of the CFS data on proton-nucleus collisions[7].

No contradiction to the scaling requirement in term of $\sqrt{\tau} = M_{\mu\mu}/s$ has emerged experimentally. This is illustrated in Figs. 16 and 17 which reproduce a compilation of the proton production data and of the results for pion production by the NA3 collaboration.

The study of the angular distribution of the lepton pairs is an interesting subject which begins to be studied with sufficient experimental accuracy to show significant deviations from the $1 + \cos^2\theta$ dependence expected for transverse virtual photon decay.

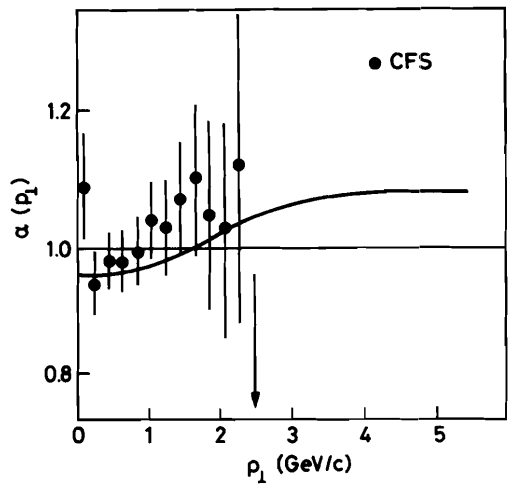

Fig. 15 P_T dependence of the α parameter, characterizing the A dependence, for $M_{\mu\mu} \sim 7$ GeV/c^2. The curve represents the calculation by C. Michael.

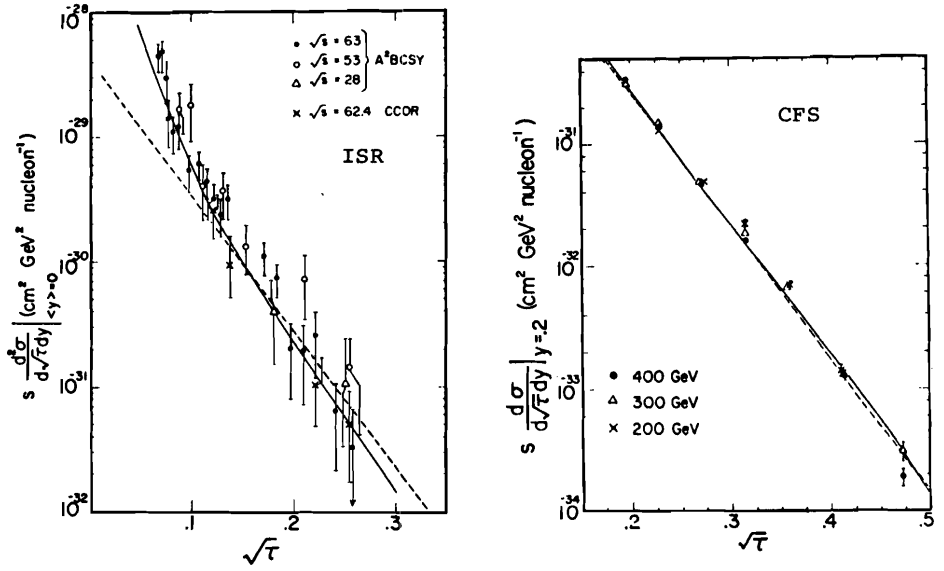

Fig. 16

The definition of the angles is illustrated in Fig. 18 and a sample of earlier results for the polar dependence is given in Fig. 19. The NA3 collaboration has collected sufficient statistics (e.g. 1.5×10^4 events with $4.5 \leq M_{\mu\mu} \leq 8.5$ GeV/c^2 with $x_{\mu\mu} > 0$ after like sign subtraction from π^-p interactions at 150 GeV/c) with reasonably flat azimuthal acceptance so that the $W(\theta,\phi)$ angular distribution can now be studied in both variables as a function of P_T.

Assuming parity conservation, one can write

$$W(\theta,\phi) \approx 1 + \cos^2\theta + A \sin^2\theta + B \sin 2\theta \cos\phi + C \sin^2\theta \cos 2\phi$$

which integrated over ϕ reduces to

$$W(\theta) \approx 1 + \lambda \cos^2\theta \text{ with } \lambda = \frac{1 - A}{1 + A}$$

The density matrix elements are connected to the coefficients of the angular distribution:

$$\rho_{00} = \frac{A}{A + 2} \; ; \quad \mathrm{Re}(\rho_{10}) = - \frac{B}{\sqrt{2}(A + 2)} \; ; \quad \rho_{1-1} = \frac{C}{A + 2}$$

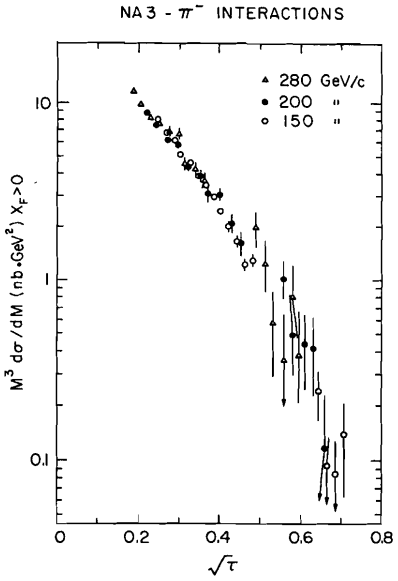

Fig. 17

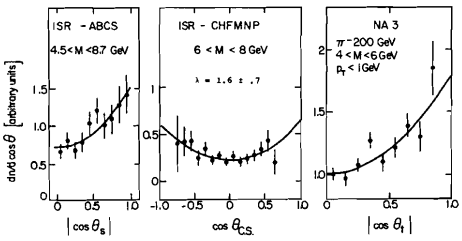

Fig. 19

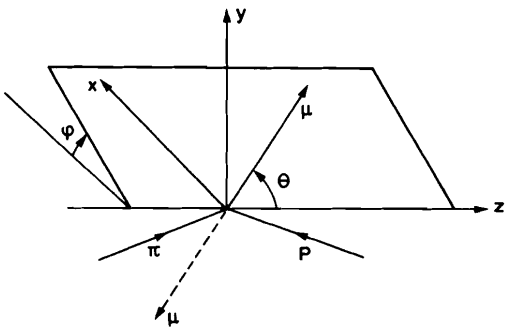

Fig. 18 Definition of frame of reference and angles.
x-z is the plane of π-p in the μμ centre-of-mass
(G-J) t-channel, z → direction of π
u-channel, z → direction of - p
(C-S) z → bisector of π and - p

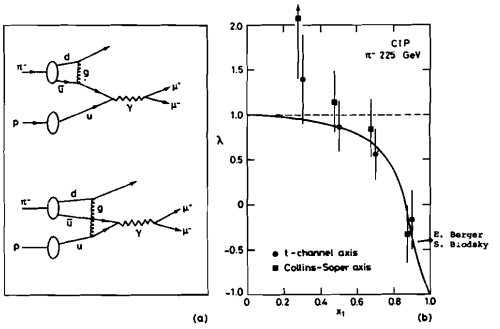

Fig. 20

Clearly for $P_T \approx 0$ there can be no azimuthal dependence and $B \approx C \approx 0$. Using specific assumptions, Berger and Brodsky[8] have computed

$$\frac{d^3\sigma}{dx_1\ d\cos\theta\ dy} \approx (1-x_1)^2\ (1+\cos^2\theta) + \frac{4}{9}\frac{P_T^2}{M_{\mu\mu}^2}\sin^2\theta + \frac{2}{3}\frac{P_T}{M_{\mu\mu}}(1-x_1)\sin 2\theta\cos\theta$$

in the t-channel frame and for the fractional momentum carried by the antiquark (or quark) in the incoming pion $x_1 \to 1$, on the basis of the higher twist contribution indicated diagrammatically in Fig. 20a. Figure 20b shows the calculated dependence of the parameter λ on x_1 and the results by the CIP collaboration. The NA3 collaboration has measured the coefficient, let us call it H, of the $(P_T/M_{\mu\mu})(1-x_1)\sin 2\theta\cos\phi$ term of the angular distribution, and found for $x_1 > .7$ (2900 eV) $H = 0.4 \pm .1$ and for $x_1 > .85$ (770 eV) $H = 0.2 \pm 1$ instead of 2/3 as computed by Berger and Brodsky. This indicates that higher twist effects are probably less important than predicted.

Integrating over $x_{\mu\mu} > 0$, the NA3 collaboration measured

$$\rho_{00} = (.9 \pm .6)\left(\frac{P_T}{M_{\mu\mu}}\right)^2 \quad \text{(compatible with 0 within the large error!)}$$

$$\rho_{1-1} = (.7 \pm .2)\left(\frac{P_T}{M_{\mu\mu}}\right)^2 ; \quad \beta_0 = (.3 \pm .2)\ \frac{P_T}{M_{\mu\mu}}$$

where β_0 is the angle of rotation between the u-frame and a frame (with the z-axis in the $\bar{q}$ direction) in which $Re(\rho_{10}) = 0$. The above values of ρ_{00} and ρ_{1-1} are given in this latter frame.

The known empirical facts about the P_T dependence of the continuum dilepton production have stimulated much fruitful theoretical thinking.

Contrary to the naive version of the Drell-Yan model, which predicts zero transverse momentum for the virtual photon, it is found that $\langle P_T \rangle$ is larger than plausible values of the intrinsic parton momentum K_T in the hadrons and that it grows with M at fixed s reaching a plateau which has a higher value for pion compared with proton induced pairs, Figs. 21 and 22.

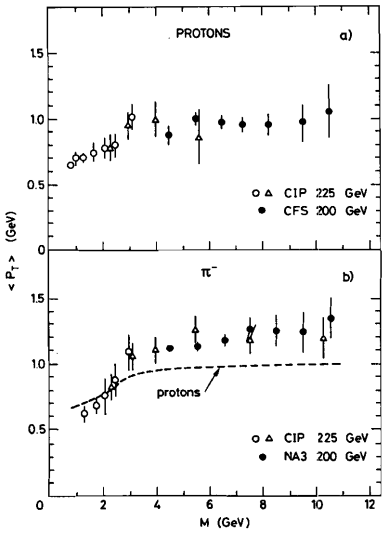

Fig. 21 Mass dependence of $\langle P_T \rangle$ for proton and pion produced μ-pairs.

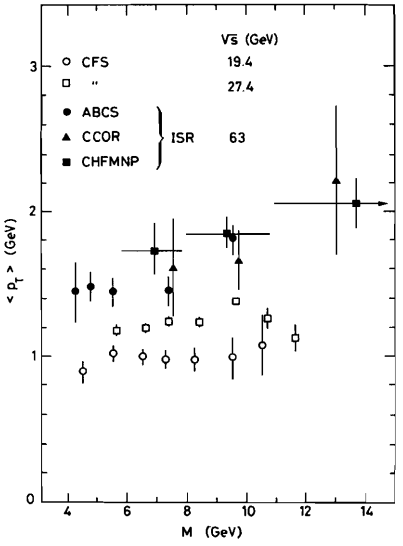

Fig. 22 Mass dependence of $\langle P_T \rangle$ for proton produced lepton pairs at FNAL and ISR.

One can express $\langle P_T^2 \rangle = \langle k_T^2 \rangle + \langle P_T^2 \rangle_{QCD}$

$$\langle P_T^2 \rangle_{QCD} = s \times f(\tau, \alpha_s(M_{\mu\mu}^2)) \cdot \alpha_s(M_{\mu\mu}^2) \quad \text{with } \tau = M_{\mu\mu}^2/s$$

Results on the s dependence at fixed $\sqrt{\tau}$, which include data at low $\sqrt{s}$ and $M_{\mu\mu}$ from the Ω collaboration[9], are illustrated in Figs. 23 and 24 for pions and protons. While a first order QCD calculation with scaling violation via the $\alpha_s(M_{\mu\mu}^2)$, dependence by J. Badier[10] fails to fit the τ dependence of the NA3 data (Fig. 25), a more refined treatment of soft gluons plus exact kinematical constraints by Chiappetta and Greco[11] gives excellent fit to the proton P_T distribution with $\langle k_T^2 \rangle \approx .4$ (GeV/c)^2.

As a conclusion to this first part of the review I would like to remark that the interplay of experimental findings and theoretical ideas has produced a remarkable progress, which is likely to continue in the near future with results from the presently running experiments at FNAL and at the CERN SPS.

Forthcoming experiments using a gas jet target for $\bar{p}$-p interactions at the SPS or exploiting higher energy beams from the FNAL Tevatron and, may be, polarized proton beams against polarized targets, could investigate qualitatively new aspects. In particular the expectation of important results at the forthcoming

colliders (CERN, FNAL, ISABELLE...) concerning new quark flavours, intermediate vector mesons, parity violating effects, etc, seem to me totally justified.

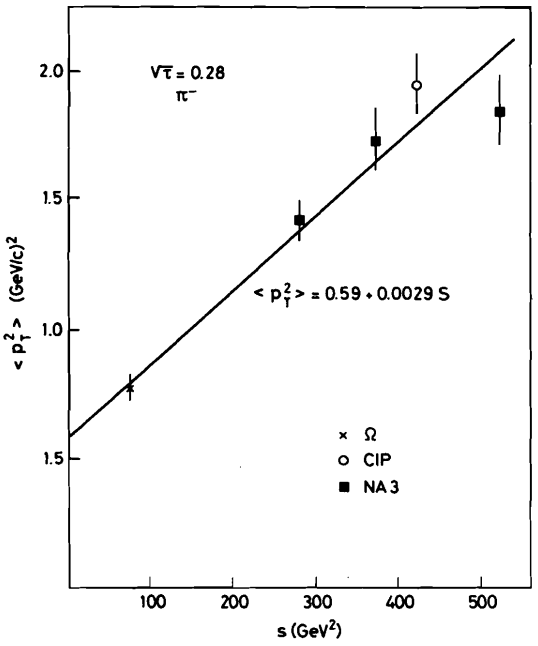

Fig. 23 s dependence of $\langle P_T^2 \rangle$ for pion-produced μ-pairs.

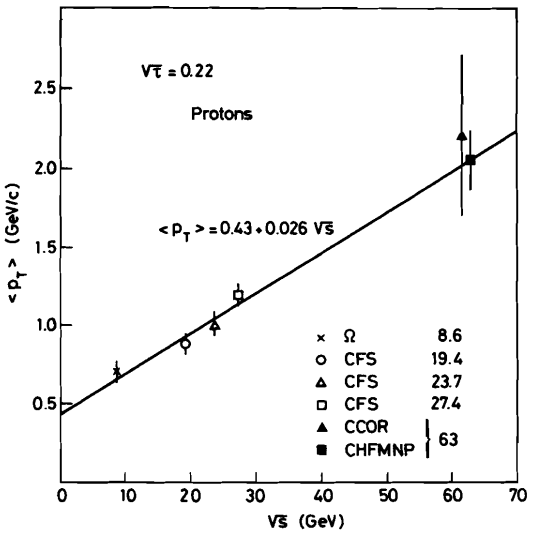

Fig. 24 s dependence of $\langle P_T \rangle$ proton-induced μ-pairs.

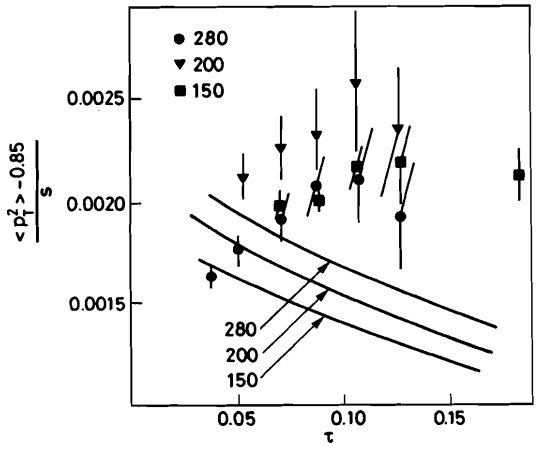

Fig. 25a The lines drawn refer to the calculations by J. Badier.

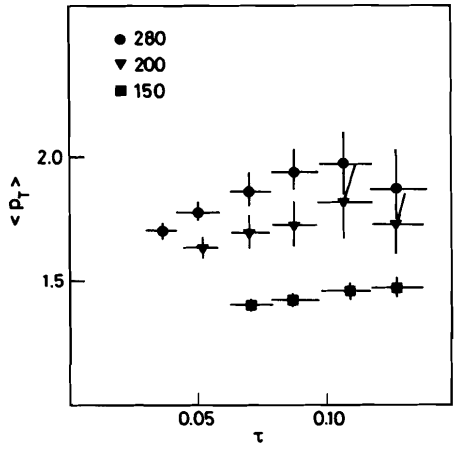

Fig. 25b

LOW MASS LEPTON PAIRS AND DIRECT PRODUCTION OF SINGLE PHOTONS

Recently additional experimental evidence has been obtained on low mass ($\lesssim$ 1 GeV/c^2) lepton pair production in hadronic interactions. This is outside the realm of application of the Drell-Yan model and is briefly reviewed here mostly because of its connection with direct single photon production. Following some early somewhat contradictory results, a number of experiments report now the observation of a sizeable dilepton signal (Fig. 26) for masses below the ρ after subtraction of direct decays and Dalitz pairs from known resonances.

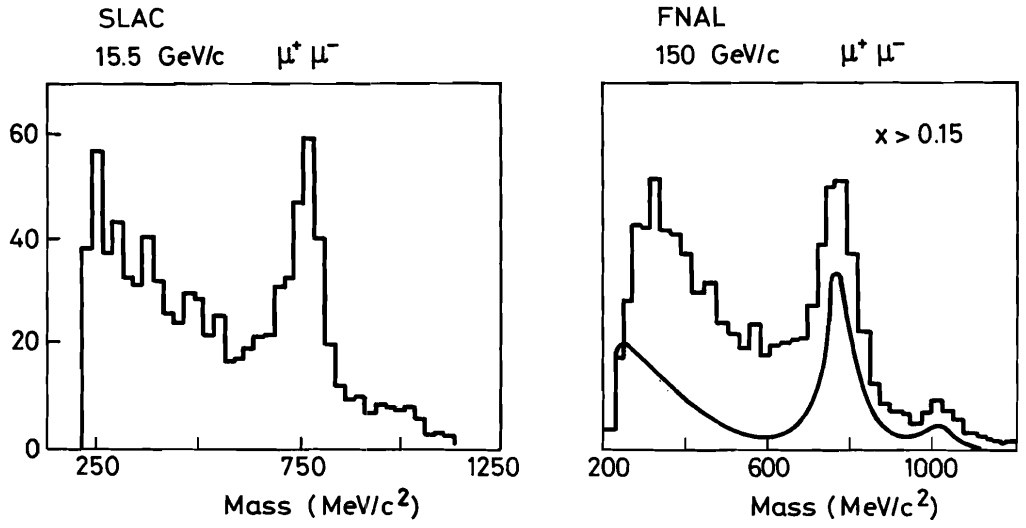

Fig. 26

A Caltech-John Hopkins-SLAC experiment using the LASS spectrometer has been performed with π^-p at 16 GeV. The mass distribution obtained is shown in Fig. 27, while in Fig. 28 the mass, x and P_T^2 distributions are plotted (before and after subtraction of Dalitz pair from η and ω) indicating a strong peaking of the signal at low x and P_T. The authors construct a model which postulates a

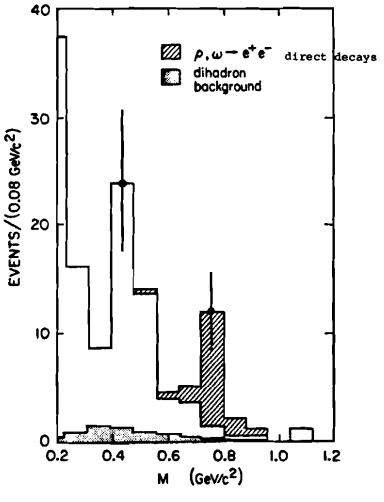

Fig. 27

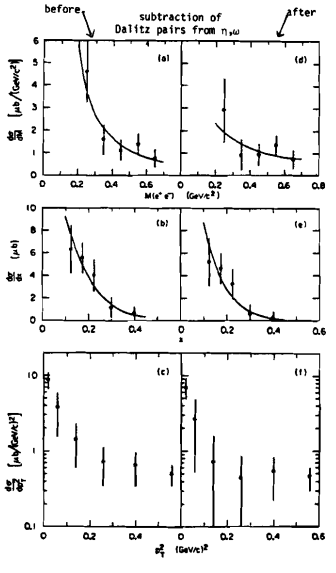

Fig. 28

Dalitz type of mechanism for $q\bar{q}$ states with $J^P = 0^-$ and masses centred in the $0.6 \div 0.9$ GeV/c^2 region. With such a model they fit their data and existing measurements of the e/π ratio.

A second experiment by the BNL-Pennsylvania-Stony Brook collaboration [13] using the MPS spectrometer, has again looked at e^+e^- pairs from 17 GeV/c π^-p interaction but detecting also with high efficiency additional associated photons and charged particles. They have used two trigger schemes: trigger A has high acceptance at high $x(\gtrsim 0.4)$ while trigger B extends to lower x values (down to ~ 0.2). In agreement with the other experiments a low mass excess of a similar magnitude is detected, only for the low x trigger B (Figs. 29 and 30). The result of the study of the associated photon multiplicity is relevant to the mechanism of production. They find that for e^+e^- masses below 0.1 GeV/c^2 an associated γ, making up the π^0 mass, is frequently present as expected for π^0 Dalitz decay. For $0.1 \lesssim M_{e^+e^-} \lesssim 0.6$ GeV/c^2 and $x < 0.5$ they find, however, (Fig. 31) no significant increase of associated photon frequency, contrary to the expectation in case the Dalitz type[12] of production mechanism were indeed dominant. Of course, whichever may be the mechanism of production of the low mass virtual photon, their presence implies the production of real photons. For e^+e^- masses $M_{e^+e^-} \gg m_e$ these processes are related by

$$\frac{d^3\sigma_{e^+e^-}}{dM_{e^+e^-}\, dx\, dP_T^2} = \frac{2}{3}\,\frac{\alpha}{\pi}\,\frac{1}{M_{e^+e^-}}\,\frac{f(M_{e^+e^-}, x, P_T^2)}{f(0, x, P_T^2)} \times \frac{d^2\sigma_\gamma}{dx\, dP_T^2}$$

where $f(M_{e^+e^-}, x, P_T^2)$ is the structure function for production of a virtual photon of mass $M_{e^+e^-}$ summed over photon polarization. With reasonable assumptions on the $M_{e^+e^-}$ dependence of $f(M_{e^+e^-}, e, P_T^2)$ (i.e. constant with M or linear M dependence) both authors predict direct single photon to pion production ratio as high as $10 \div 20\%$ for $P_T \lesssim 1$ GeV/c.

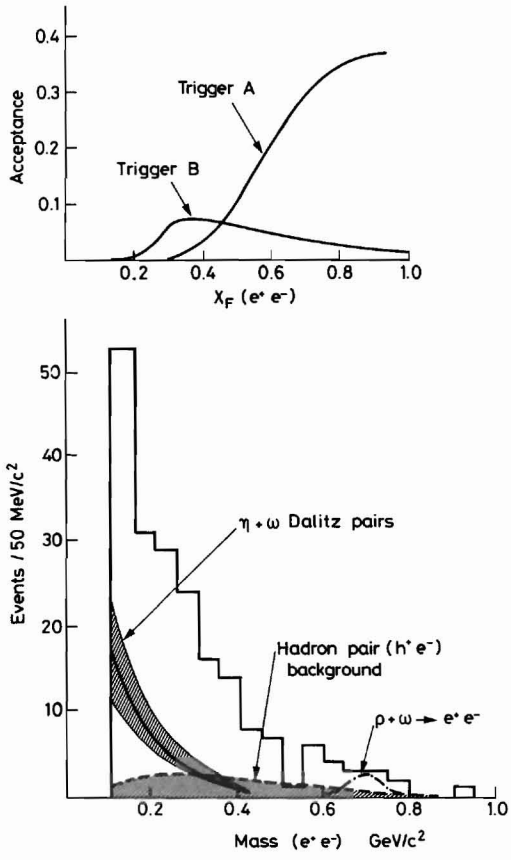

Fig. 29

Previous results at the ISR[14] also measuring low mass electron pairs, had, on the contrary, given an upper limit for the direct single photon to pion production ratio at $2 \lesssim P_T \lesssim 3$ GeV/c of $1 \div 2\%$, which still to-day represents the most accurate $1\gamma/\pi^0$ experimental value.

Due to the difficulty of triggering on low mass lepton pairs at high P_T and to the large reduction in cross section going from real to virtual photons, it has not been possible to push the measurements to higher P_T values. In spite of the very serious background problems when selecting real photons it has been found necessary to switch to them in order to measure $1\gamma/\pi^0$ for $P_T \gtrsim 3$ GeV/c. These problems are well illustrated by the results of the FNAL-John Hopkins University experiment[15] which used two Pb-glass matrices each with 25 counters 6.5×6.5 cm^2 in cross section.

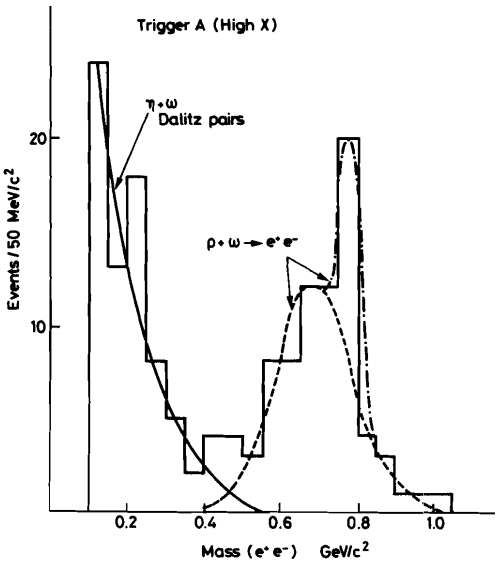

Fig. 30

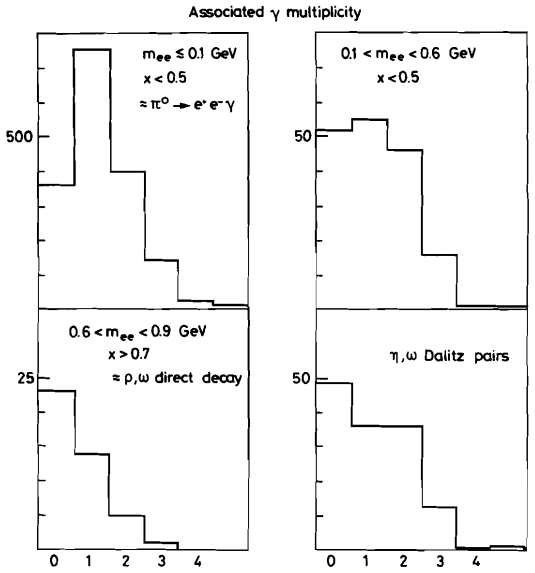

Fig. 31 Frequency distribution for the number of photons associated with e^+e^- pairs of different mass.

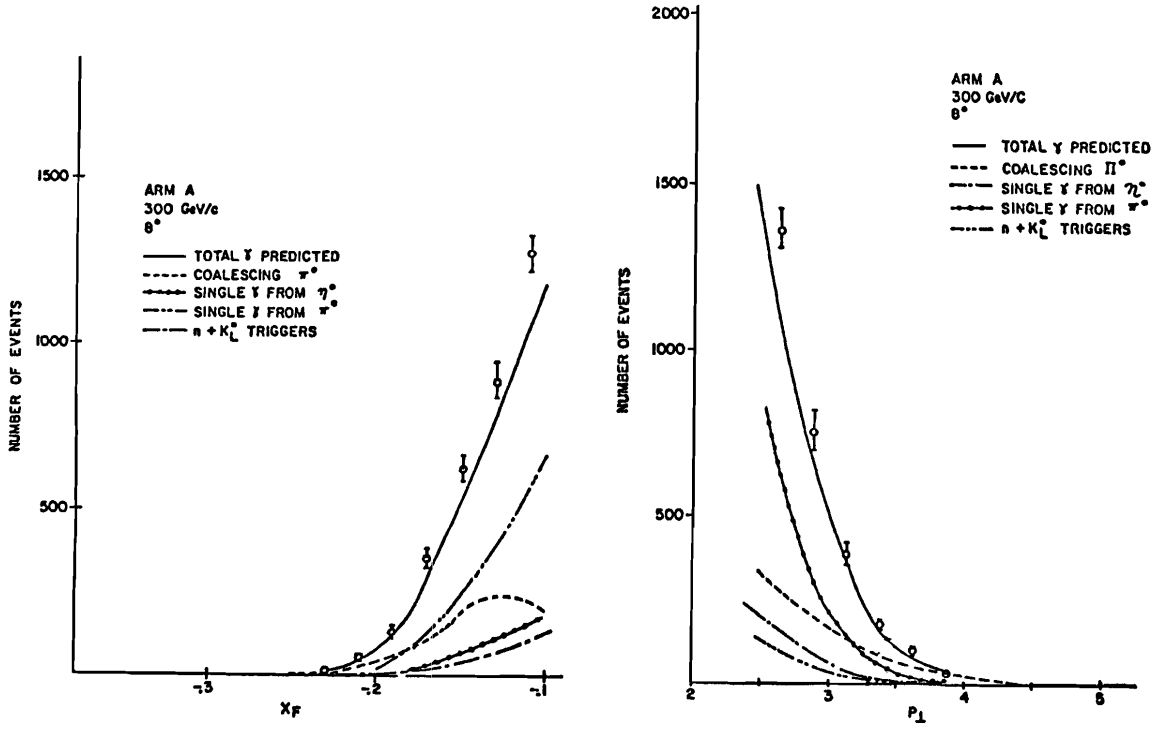

Fig. 32

Figure 32 shows, as a function of P_T and x the number of detected events and the estimated background from various sources. The subtraction amounts typically to 90% of the raw signal, hence even a relatively small systematic error in the background evaluation can change in an important way the results (shaded band in Fig. 33).

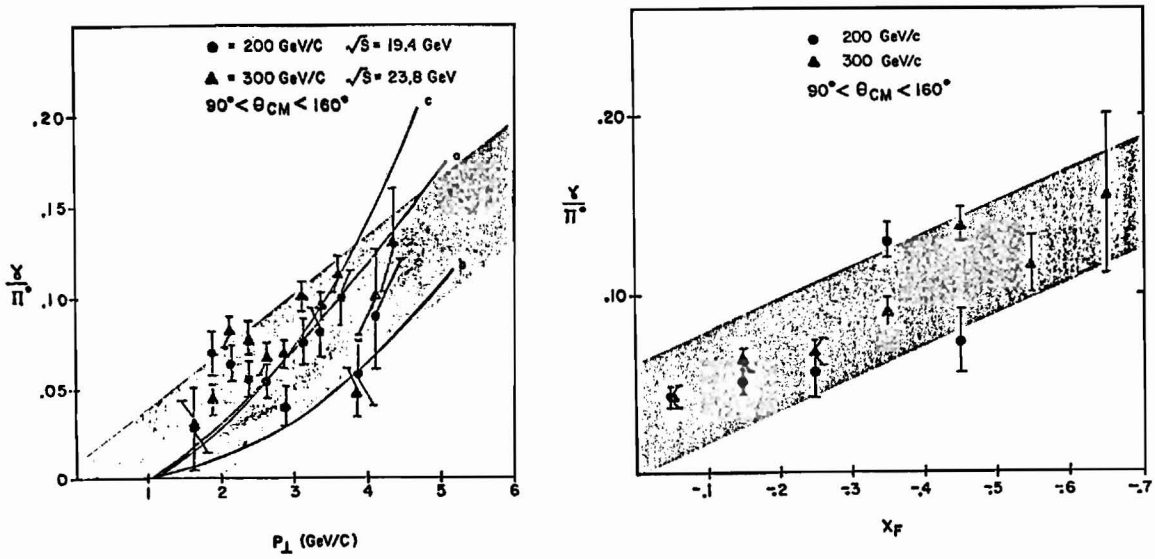

Fig. 33

I will now summarize the motivations which have induced a number of teams to try and overcome the experimental difficulties connected with the detection of high P_T direct single photon production.

The simplest QCD diagrams are illustrated in Fig. 34. The first important remark is that photons directly produced in hard collisions among the constituents carry the full transverse momentum of the interaction while a hadron. e.g. a neutral pion, with the same P_T would in general be part of a jet and as such it would have been originated in an interaction characterized by a higher P_T. Given the steepness of the P_T dependence it is quite conceivable that in this way the smallness of the electromagnetic coupling constant relative to α_s is compensated and the ratio γ/π^0 at a fixed high P_T turns out to be much larger than α.

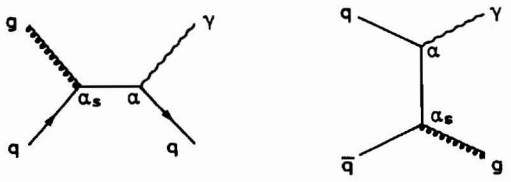

Fig. 34 The "QCD Compton" and "$q\bar{q}$ annihilation".

The first diagram "QCD Compton" is expected to be dominant in proton-proton collisions, where no valence antiquarks are available. Taken by itself, it would give the same contribution for $\bar{p}$-p interactions and for π^--p relative to π^+-p.

The second diagram "$q\bar{q}$ annihilation" is expected to be dominant in presence of valence antiquarks. Its contribution would be much larger in $\bar{p}$-p compared to p-p and (due to the ratio of the charges of valence antiquark) in π^-p compared to π^+p. Also the recoil jet on the opposite side of the higher P_T direct single γ is of the q type in the first case (QCD Compton) and of g type in the in second ($q\bar{q}$ annihilation). If one could isolate the two diagrams, e.g. by a suitable choice of the kinematical conditions, then one would look separately at jets from quark or from gluon fragmentation. In p-p interactions u quarks are twice as

frequent as d quarks and since the probability of photon emission goes with the square of the electric charge, recoil jets from u quarks should be about eight times more frequent than jets from d quarks. This should be reflected in the frequency of positively versus negatively charged particles, especially for particles carrying a P_T approaching the P_T of the γ in the direction opposite to it. Figure 35 gives an example of calculation of the charge frequency ratio by Holzen and Scott[16].

Of course, in the case of $q\bar{q}$ annihilation, the recoil jet being from gluon fragmentation, the particle frequency does not depend on the sign of the charge. In both cases the direct single photon is not part of a jet and hence it is expected to come "unaccompanied".

It is clear, however, that the photon could also be produced by quark bremsstrahlung. In this case (Fig. 36) it is expected to come "accompanied" by the particles from the quark fragmentation (again charge 2/3 quarks favoured). The bremsstrahlung contribution is computed to be relatively more important for large longitudinal momenta and its study is quite interesting in view of extracting information on the 3-gluon vertex.

In analogy to the Drell-Yan case, higher order QCD contributions are quite important. Taking appropriately into account emission and exchange of gluons[17] modifies the naive expectation by a multiplicative factor $K' \simeq 1.7$. In addition, higher twist effects have been calculated not to be negligible, although their size is not yet well established.

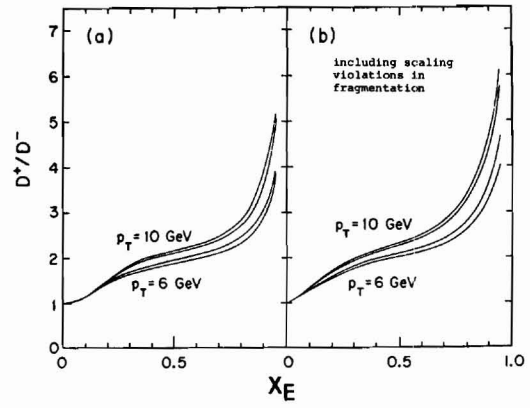

Fig. 35 Ratio of frenquency of positive/negative particles in the jet opposite the high P_T photon as a function of X_E. X_E is the ratio of the P_T of the particle, projected in the direction opposite to the photon, to the P_T of the photon.

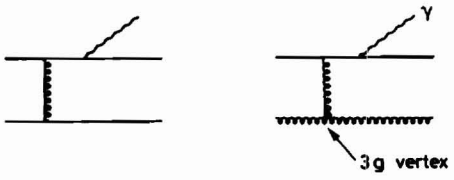

Fig. 36 Simplest QCD diagrams for production of high P_T photons by quark bremsstrahlung

Going now to review experimental results, I would like to mention the two experiments which up to now have provided most of the available data on direct single photon production in hadronic interactions. Both experiments have used the CERN ISR. The R108 collaboration detects photons in two large arrays of Pb-glass counters (Fig. 37) which, however, do not have sufficient granularity to resolve photon pairs from π^0 decay at high P_T.

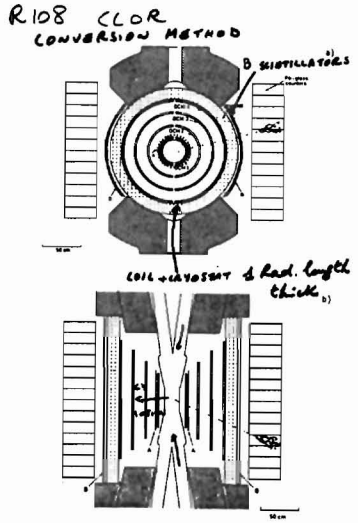

Fig. 37

The interaction point is surrounded by a drift chamber system in the field of a superconducting solenoid, with a coil plus cryostat thickness of 1 radiation length. Scintillation counters outside the coil signal the conversion of neutral showers. The fraction of non converting neutral showers is expected to be about 50% in case of single photons and about 25% in case of two overlapping γ from a π^0. The method is sensitive only when $\gamma/\pi^0 \gtrsim 10\%$ and has required an assumption on the value of γ/π^0 for P_T below 5 GeV/c. A clear single photon signal is detected (Fig. 38) above 6 GeV/c. The ratio of single photons to all neutral showers has been measured (Fig. 39) separately for "accompanied" and "unaccompanied" showers. For P_T < 10 GeV/c it would appear that essentially all single γ are indeed produced in isolation and not as part of a jet, while a sizeable contribution from quark bremsstrahlung could be present at higher P_T.

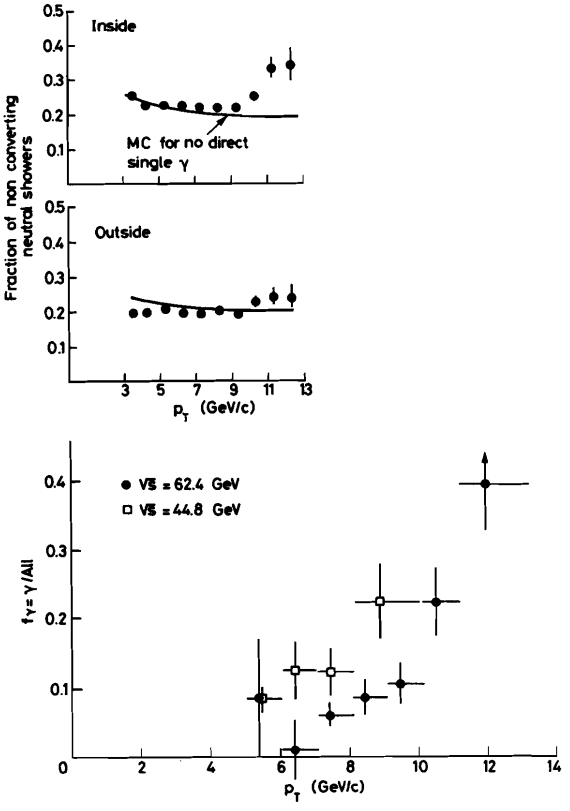

Fig. 38

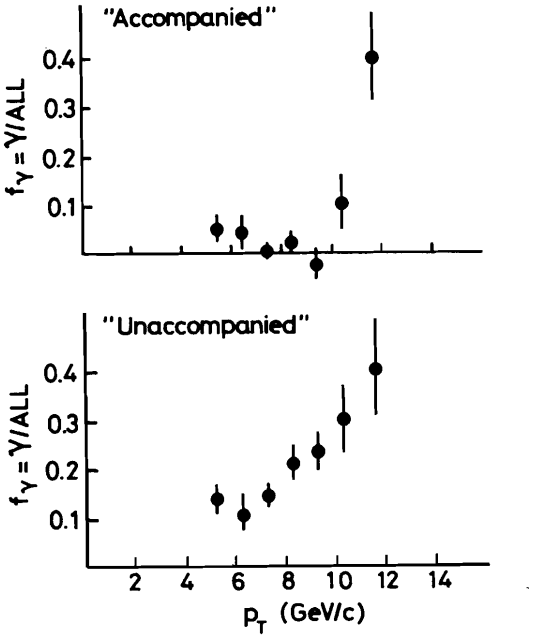

Fig. 39

A study of the $R^{\pm}$ ratio of the frequency of positive versus negative particles in the side opposite to the single photon candidates has been carried out[18] (Fig. 40). The single photon component is enhanced in the sample of unaccompanied and non coverting showers compared with the sample of accompanied and converting showers. The errors are large but the tendency is qualitatively as expected in favour of a higher frequency of positive high P_T particles.

The other ISR experiment, R806, has used liquid argon calorimeters in different geometrical arrangements, Fig. 41[19]. The transverse and longitudinal subdivision of the calorimeters allow to resolve efficiently showers 4 cm away from each other. Given their excellent stability and linearity of response, it has been possible to simulate reliably their performance, including the efficiency of the

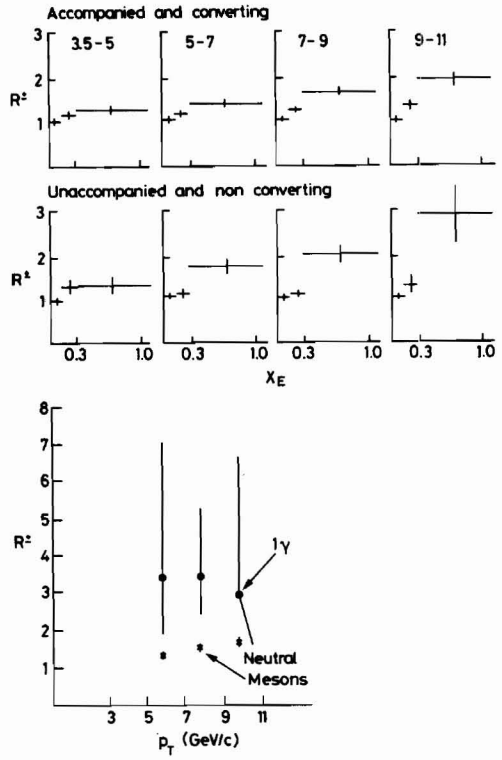

Fig. 40

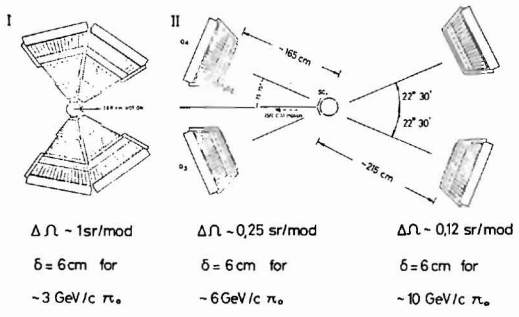

Fig. 41 R806 experimental set-up.

reconstruction program, using the EGS[20] Monte Carlo, as demonstrated by a number of direct experimental checks.

A sample of results for γ/π^0 at different ISR energies[21] is shown in Fig. 42. The lines drawn correspond to the calculation by A.P. Contogouris[17]. The full line includes the K' factor.

The analysis of a new higher statistics run has recently been completed, extending the P_T range up to 12 GeV/c. The raw γ/π^0 ratio is shown in Fig. 43. The data points are shown with the statistical error and with the systematic error due to a possible non-linearity combined with it. The level of background and its estimated uncertainty is also shown. Finally, in Fig. 44 the new results for the corrected γ/π^0 are plotted with their full errors and compared with the previous results at $\sqrt{s}$ = 63 GeV. The two sets of data are clearly in excellent agreement.

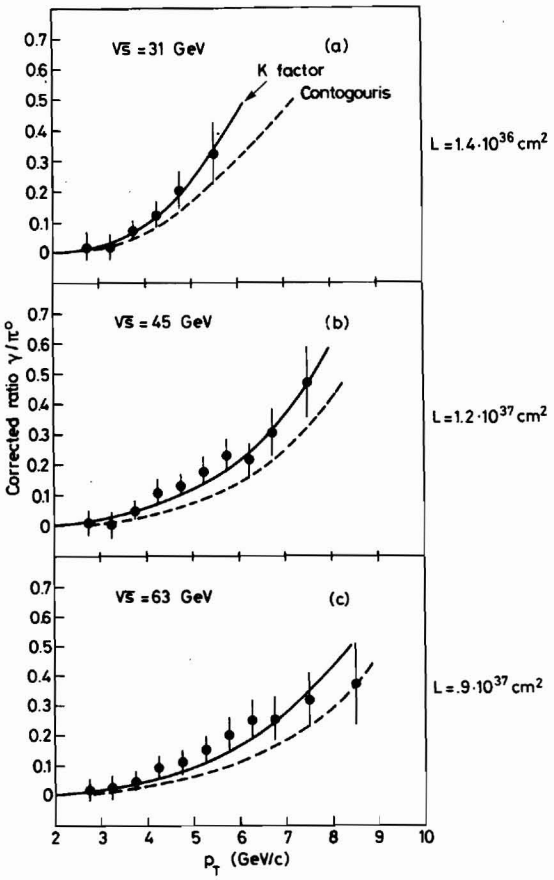

Fig. 42

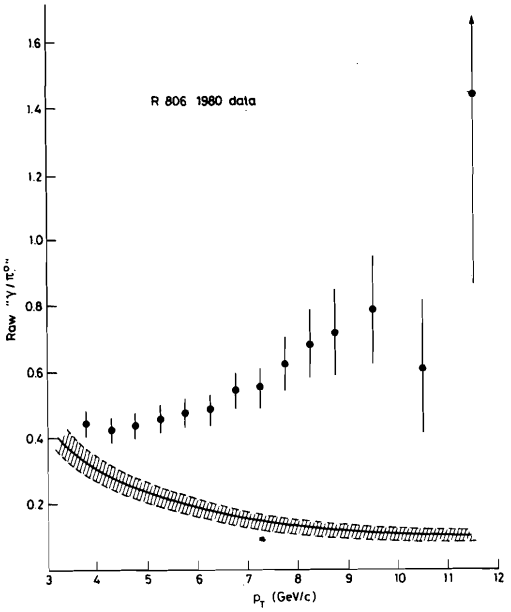

Fig. 43

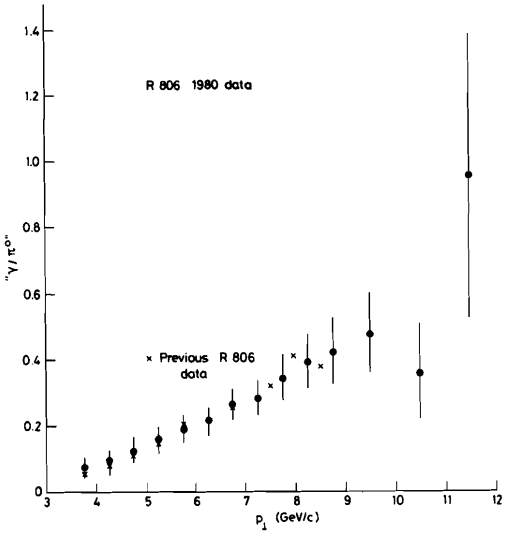

Fig. 44

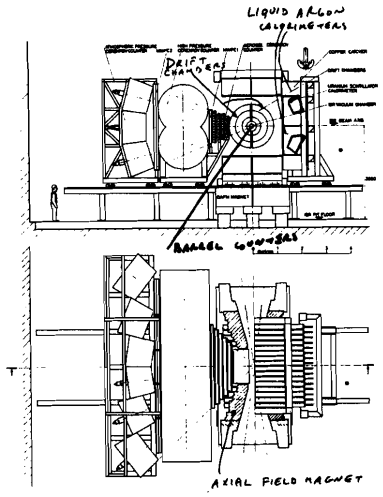

Fig. 45 R807 - A study of large transverse momentum phenomena.

More recently, data were taken with two liquid argon calorimeters incorporated in the Axial Field Spectrometer (Fig. 45), which in particular includes a set of 44 barrel counters surrounding the interaction region and a cylindrical bicycle-wheel type of drift chamber which allow to study the charged tracks produced in the same event as the high P_T direct single photon or neutral pion trigger. Figures 46 and 47 show the tracks reconstructed in the drift chambers in correspondence with two such events. In Fig. 48 results are shown on the azimuthal correlation between the trigger particle ($P_T \geq 4.5$ GeV/c, rapidity $|y| \approx 0$) and particles (of either sign) with $P_T \geq 1$ GeV/c and $|y| \leq 0.8$. No appreciable difference is seen between single photon and neutral pion trigger in the opposite side jet. On the same side, however, the photons are less frequently accompanied by charged particles, compared with the neutral pions, as indeed expected on the basis of the production mechanism, as previously illustrated.

The ratio N_+/N_- of the frequency of positive particles over the frequency of negative particles as a function of x_E (i.e. their transverse momentum projected in the direction opposite the trigger and normalized to it) is plotted in Figs. 49a and 50 for the opposite and same side respectively. In Fig. 49b N_+/N_- is plotted only for "γ unaccompanied" (defined as not having charge particles on the same side carrying in total more than 20% of the transverse momentum of the trigger) in an effort to reject photons from quark bremsstrahlung. In this case the general tendency for single photon trigger to have N_+/N_- larger than for neutral pion trigger

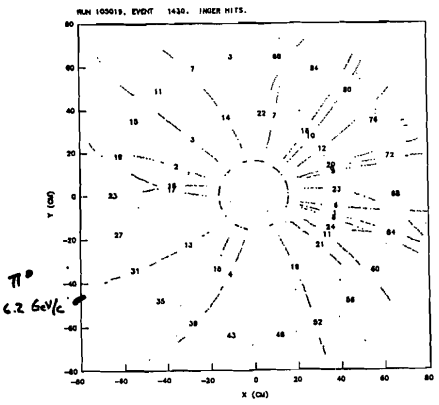

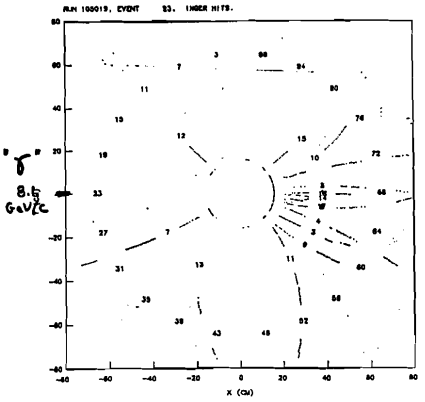

Fig. 46 Fig. 47

Charged tracks seen in the R807 cylindrical drift chamber in correspondence to a high P_T π^0 or a high P_T direct single γ.

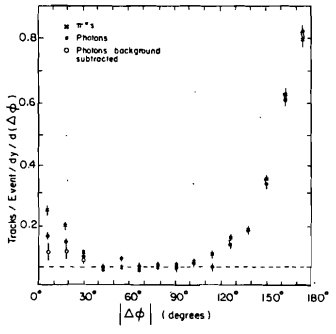

Fig. 48 R806/807 results on azimuthal correlation.

is clearly more evident and significant. However, as in the case of R108, the statistics is not yet sufficient to draw quantitative conclusions on the charge correlation.

Data of better statistical accuracy and quality should become available in the next few years from the ISR and from fixed target experiments at FNAL and CERN. At the ISR the R108/110 experiment is expected to continue with some improvement and extra active converters in front of the Pb-glass walls. R806/807 is taking additional data on charge correlation and it now includes a highly segmented hexagonal uranium scintillator calorimeter in the forward direction, specifically to enhance quark bremsstrahlung contributions. A new R808 experiment has been approved for which an active NaI converter composed of 1000 counters in front of the R807 uranium calorimeters should allow a drastic reduction of background. It is hence expected to extend the measurements of the P_T range below 3.5 GeV/c where the direct photon signal is known to be small. At least up to moderate P_T a very interesting comparison should be possible at the ISR between $\bar{p}$-p and p-p direct photon production.

An experiment at the CERN SPS using a gas jet target for $\bar{p}$-p collisions should have a much higher luminosity but a somewhat lower $\sqrt{s}$.

Conventional fixed target beams with p, $\bar{p}$, π^+, π^- will be used at FNAL and CERN by several experiments in preparation or already being set up.

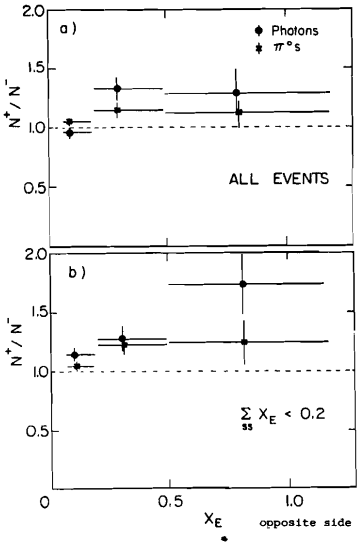

Fig. 49a Results of R806/807 on ratio frequency of positive and negative particles opposite the high P_T π^0 or γ trigger.

Fig. 49b Same as Fig. 49a but for "γ unaccompanied" trigger.

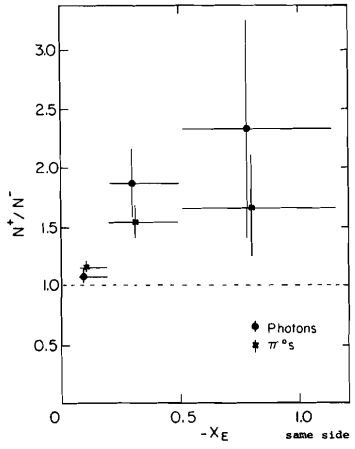

Fig. 50 Same as Fig. 49a but for particles on the same side as the trigger.

Finally, a preliminary analysis of data taken by R806 [22], with four calorimeters close to the intersection region, indicates that sufficient background rejection can be achieved in studying $\gamma\gamma$ pairs of large invariant mass (Fig. 51), a process directly related to the Drell-Yan lepton pair production (the cross section for $\gamma\gamma$ pair depending on the 4th power of the electric charge of the annihilating quarks versus the second power for Drell-Yan) and to the $\gamma\gamma$ physics which begins to be studied at high energy e^+e^- storage rings like PETRA.

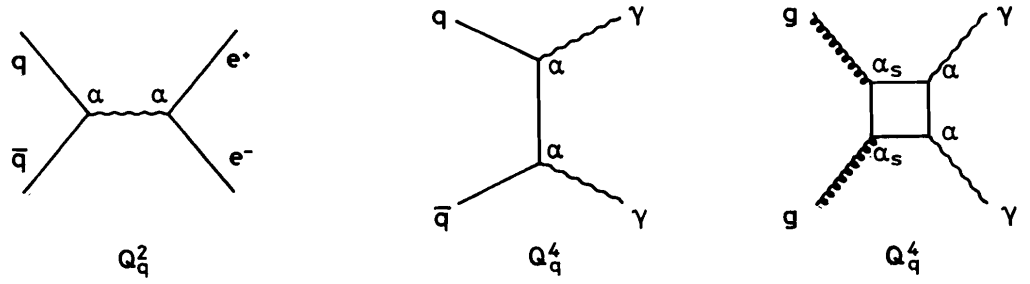

Fig. 51 Drell-Yan diagram and the simplest QCD diagram for production of large mass $\gamma\gamma$ pairs.

ACKNOWLEDGEMENT

I should like to thank Mrs. A.M. Bugge for her patience and helpfulness in preparing this paper.

REFERENCES

(1) S. Drell and T.M. Yan, Phys.Rev.Lett. 25 (1970) 316 and
Ann.Phys. USA 66 (1971) 578.
For recent reviews see for example:
G. Matthiae, Riv. Nuovo Cimento 4 No 3 (1981) and
A. Michelini, rapporteur talk at The EPS Int. Conf. on HEP Lisbon 1981.

(2) R.C. Hwa et al., Z.Phys. C1 (1979) 279.

(3) See for example:
H.D. Politzer, Phys.Rev. 14C (1974) 129.
A.J. Buras, Rev.Mod.Phys. 52 (1980) 199 and his talk on Perturbative QCD at this Symposium.
A.P. Contogouris et al., Phys.Lett. 104B (1981) 70.

(4) S.R. Smith et al., Phys.Rev.Lett. 46 (1981) 1607.

(5) The experimental results are identified by the following acronyms:

CIP	- Chicago-Illinois-Princeton	FNAL
CFS	- Columbia-FNAL-Stony Brook	FNAL
CP	- Chicago-Princeton	FNAL
NA3	- CERN-Collège de France-Orsay-Ecole Polytechnique-Saclay	CERN SPS
NA10	- Ecole Polytechnique-Strasbourg-Zürich	CERN SPS
R108 ≡ CCOR	- CERN-Columbia-Oxford-Rutherford	CERN ISR
R209 ≡ CHFMNP	- CERN-Harvard-Frascati -MIT-Napoli-Pisa	CERN ISR
R806 ≡ ABCSY	- Athens-Brookhaven-CERN-Syracuse-Yale	CERN ISR
CJHS	- Caltech-John Hopkins-SLAC	SLAC
BPS	- Brookhaven-Pennsylvania-Stony Brook	BNL

(6) C. Michael, Lepton pair production, contribution to parallel session P1, The EPS Int. Conf. on HEP Lisbon 1981 and Liverpool University preprint CTH 63.

(7) A.S. Ito et al., Phys.Rev. 23D (1981) 604.

(8) E.L. Berger, Z.Phys. C4 (1980) 289 and
E.L. Berger and S.J. Brodsky, Phys.Rev.Lett. 42 (1979) 940 and
Phys.Rev.Lett. 43 (1979) 1219.

(9) M. Corden et al., contributed paper No. 129.

(10) J. Badier, Transverse momentum of dileptons, Moriond (1981).

(11) A. Chiappetta and M. Greco, contributed paper No. 199.

(12) R. Stroynowcki et al., Phys.Lett. 97B (1980) 315.
D. Blockus et al., contributed paper No. 140.

(13) J. Stekas et al., contributed paper No. 236.

(14) A. Chilingarou et al., Nucl.Phys. B151 (1979) 29 and
J. Cobb et al., Phys.Lett. 78B (1978) 519.

(15) B. Cox, Proc. 1979 Int. Symp. on Lepton and Photon Interactions at High Energies, FNAL (1979) 602.

(16) F. Halzen and D.M. Scott, Univ. of Wisconsin preprint COO-881-140.

(17) See for example:
A.P. Contogouris et al., Nucl.Phys. B179 (1981) 461 and
Phys.Lett. 104B (1981) 70.

(18) A. Angelis et al., Phys.Lett. 94B (1980) 106 and Phys.Lett. 98B (1981) 115.

(19) J.H. Cobb et al., Nucl.Instr. Meth. 158 (1979) 93.

(20) R.L. Ford and W.R. Nelson, SLAC report 210 (1978).

(21) M. Diakonou et al., Phys.Lett. 87B (1979) 292 and Phys.Lett. 91B (1980) 296.

(22) J. Stumer, Brookhaven National Laboratory, private communication.